Cellulose (2011) 18:1151–1163
DOI 10.1007/s10570-011-9575-2

Liquid crystalline cellulosic elastomers: free standing anisotropic films under stretching

C. Sena · M. H. Godinho · C. L. P. Oliveira · A. M. Figueiredo Neto

Received: 17 May 2011 / Accepted: 5 July 2011 / Published online: 14 July 2011

Abstract The structure and local ordering of 1,6-hexamethylenediisocyanate-(acetoxypropy1) cellulose (HDI-APC) liquid crystalline elastomer thin films are investigated by using X-ray diffraction and scattering techniques. Optical microscopy and mechanical essays are performed to complement the investigation. The study is performed in films subjected or not to an uniaxial stress. Our results indicate that the film is constituted by a bundle of helicoidal fiber-like structure, where the cellobiose block spins around the axis of the fiber, like a string-structure in a smectic-like packing, with the pitch defined by a smectic-like layer. The fibers are in average perpendicular to the smectic-like planes. Without the stretch, these bundles are warped, only with a residual orientation along the casting direction. The stretch orients the bundles along it, increasing the smectic-like and the nematic-like ordering of the fibers. Under stress, the network of molecules which connects the cellobiose blocs and forms the cellulosic matrix tends to organize their links in a hexagonal-like structure with lattice parameter commensurate to the smectic-like structure.

C. Sena (✉) · C. L. P. Oliveira · A. M. Figueiredo Neto
Instituto de Física, Universidade de São Paulo, Caixa Postal 66318, São Paulo, São Paulo 05314-970, Brazil
e-mail: cleidios@if.usp.br

M. H. Godinho
Faculdade de Ciências e Tecnologia e CENIMAT/I3N, Universidade Nova de Lisboa, Quinta da Torre, 2829-519 Caparica, Portugal

Keywords Liquid crystalline cellulose film · Structure · Orientational order parameter · Birefringence

Introduction

Cellulose and their derivatives attract the attention of researchers due to their outstanding physical–chemical properties (Kolpak and Blackwell 1976). In nature it is abundant, presents renewability, low cost and availability. Their different preparation methods generate materials with different mechanical, optical, thermal and structural properties (Siqueira et al. 2010). Because of this, cellulose derivative have been widely used as reinforcing agents in bio and nano composites (Liu et al. 2011; Siqueira et al. 2010), electro-optical displays materials (Godinho et al. 1998; Almeida et al. 2002; Costa et al. 2007), local strain sensor (Almeida et al. 2009) and biocarrier.

Cellulose derivatives such as (acetoxypropy1) cellulose (APC) can form lyotropic and thermotropic cholesteric phases. The pitch of the helicoidal structure in the liquid crystalline solutions, with organic solvents, can be varied by changing the polymer concentration (Tseng et al. 1981). It is well established that application of a shear flow in this solutions can induce an unwinding of the cholesteric helix and hence a cholesteric-to-nematic transition (Andresen and Mitchell 1998). During the film preparation, the flow

of the liquid crystal state under shear stress can induce on it anisotropic mechanical properties (Andresen and Mitchell 1998), reflecting the state of molecular orientation. The films are brittle when stretched parallel to the shear direction, and ductile when stretched perpendicular to it. The component of the precursor solutions strongly influences the mechanical properties of the APC composite films (Filip et al. 2006). The APC has higher flexibility than the other liquid crystalline polymers (LCPs) such as hydroxypropylcellulose (HPC) and poly-benzyl-L-glutamate (PBLG) (Cidade and Leal 2003). Because of their topological symmetry, the molecules of the LPCs are easily oriented in large domains during the shear flow, and an additional elastic energy is stored in the polymer solution. When the shear stops, the oriented polymer chains will first relax, but, due the highly concentrated and aligned rigid chains in domains, the polymer chains cannot relax individually. This produces an internal stress that induces a periodical contraction, resulting in a banded (stripes) texture. These textures are frequently observed, by AFM and optical microscopy, in both thermotropic and lyotropic LPCs. These stripes appear perpendicular to the shear direction, and represent a periodic variation of the director around the direction of the shear. The precursor solution composition, solvent evaporation time, film thickness, rate and shear duration strongly influences the morphology of the striped texture (Godinho et al. 2002; Wang and Labes 1992; Mori et al. 1999).

Deuterium NMR experiments were used to analyze the distribution of director orientation in electro-spun microfibers, thin film and bulk samples made with liquid crystalline APC and a deuterated nematic 4-pentyl-4-cyanobiphenyl (5CB-αd_2). It was observed that the 5CB probe molecules separate out of the network and concentrate in small droplets. In thin film samples, these droplets showed a nematic-to-isotropic transition (Kundu et al. 2010). The introduction of dispersed silica nanoparticles in HPC and hydroxyethylcellulose (HEC) films results in structural changes. An ordered liquid-crystalline microfibril phase is formed, with a structural parameter typical of hexagonally packed rods (average center to center distance of 12.8 Å) (Evmenenko et al. 2004b).

In the case of HDI-APC elastomers in thin films, a uniaxial stretch applied along the director direction induces a continuous increase of the nematic director order. When the stretch is applied perpendicular to the director, a decreasing of the orientational order occurs until reaches an isotropic state. After that, the order increases again, with the director oriented at 90° with respect to the former direction the initial direction (Godinho et al. 2009). This behavior was theoretically treated by Bladon et al. (1994).

It is known that APC chains in thin films have a lateral repeating distance of ~11.3 Å (Godinho et al. 2009; Evmenenko et al. 2004a), however, a more extensive investigation of the local structure of these derivatives was still to be done. In this paper we make a deep X-ray diffraction and scattering investigation of the local ordering and structure of these HDI-APC elastomers in thin films. Mechanical and optical microscopy assays complement this study with the 0.5% HDI/70% APC elastomers thin free-standing films. The study is performed with the films initially in the relaxed state, during and after a mechanical uniaxial stress applied along or perpendicular the casting direction, and under relaxation.

Experimental

Sample preparation

The synthesis of (Acetoxypropyl) cellulose (APC) was made in accordance with the procedure described in literature (Costa et al. 2007; Godinho et al. 2009). First the acetylation of (hydroxypropyl) cellulose (HPC) (Aldrich, nominal Mw = 1,00,000) (molar substitution equal to 3.5 determined by NMR1H) (50 g) was performed with acetic anhydride (160 g) in the presence of acid acetic (15 g). APC was obtained by precipitation in water, then purified by dissolving in acetone, and finally reprecipitation in water. The final product was dried in an oven at 60 °C, the final yield was around 80%. The number of acetyl groups per residue was evaluated by NMR1H and was 2.2. A chiral nematic solution was obtained, in a 5 ml container, by adding APC to dimethylacetamide (DMAc) (Merck) (60% w/w), at room temperature, which was allowed to mix for several weeks. The APC was then lightly crosslinked with 1, 6-hexamethylenediisocyanate (HDI) (Aldrich) (0.5% calculated from the fraction of esterification), under nitrogen atmosphere. In this stage the viscous cholesteric phase was well stirred in order to obtain a homogeneous solution. To prepare the thin films, a

Gardner casting knife moving with a controlled speed of 5 mm/s was used to spread the liquid crystalline solution onto a Teflon plate (Godinho et al. 2002). The sheared casted solutions were stored at room temperature for about 2 weeks to complete the cross-linking and dried. Due to the cross-link and the high viscosity of the polymer solution the shear alignment induced a cholesteric to nematic transition which was preserved in the films after solvent evaporation, at room temperature. The final dried films were found to have an average thickness varying from 20 ± 2 to 30 ± 2 μm.

X-ray diffraction setup

The X-rays experiments were performed in the Laue geometry, using a NanoStar diffractometer from Bruker Instruments. The samples were placed in a vacuum chamber, with a micrometric stretching device. The collimation system consists of three pinholes of 750, 400 and 1,000 μm diameter, successively disposed in the beam direction. The monochromatic X-ray ($\lambda_x = 0.154$ nm) beam was oriented along the z-axis of the laboratory frame, perpendicular to the biggest sample surface area. The experiments were performed at room temperature ($\sim 23 \pm 1$ °C). The wide angle diffractograms were recorded in image plates placed at 5 cm from the sample position and after digitized. The experimental resolution, obtained from the width at half-height of a Bragg peak from a single crystal, is $0.38 \pm 0.01°$. The scattering vector modulus is defined as $q = (4\pi\sin\theta)/\lambda_x$, where 2θ is the scattering angle. The samples are rectangular films 21 μm thick, with ($L_0 = 2$ mm) × 5 mm of free surface. The relative uniaxial stretch of the sample is defined as $\varepsilon = \Delta L/L_0$, where $\Delta L = L - L_0$, L_0 and L are the length of the sample unstretched and under stress, respectively.

For some cases, Small Angle X-Ray scattering experiments (SAXS) were performed on the same conditions. The data is collected on a two-dimensional detector placed at 60 cm from the sample position. In this case the scattering pattern is isotropic with respect to the azimuthal angle and therefore the full circle is integrated, independently to the film stretching direction. As will be shown, the combination of wide angle and small angle results information provided complementary information.

Mechanical setup

Samples were rectangular films 21 μm thick, with 15 mm × 5 mm of free surface, investigated by using a universal testing system (Instron 3369), at room temperature. The uniaxial stretched was applied at a rate of 20 mm per minute, along the longest sample dimension. Five independent successful measurements were performed with the longest dimension of the sample parallel or perpendicular to the casting shear direction. The features (not the values) of the stress/strain curves obtained were similar to those from other APC and HPC already reported in the literature (Borges et al. 2001; Almeida et al. 2009).

Optical microscopy setup

We employed a Leitz polarized light optical microscope in the transmission-light geometry, at room temperature. Samples were rectangular films 21 μm thick, with 2 mm × 5 mm of free surface. They were uniaxially stretched (at 2 mm/s) along or perpendicular to the casting direction and left to relax as a function of time.

Results and discussion

The X-ray assays

Unstretched film

The X-ray diffraction patterns of the free standing, unstretched, cellulose films present three diffraction peaks, anisotropically disposed around the z-axis, as shown in Fig. 1. In Fig. 2a, b the diffracted intensity is plotted as a function of q, along the x and y axes directions. The diffraction peaks in the curves $I \times q$ were fitted with Lorentzian functions to find the characteristic distances (d) and full-widths at half-height (W). The characteristic distances associated to the peaks are $d_1 = (11.3 \pm 0.2) \times 10^{-1}$ nm, $d_2 = (4.4 \pm 0.1) \times 10^{-1}$ nm and $d_3 = (5.0 \pm 0.1) \times 10^{-1}$ nm. In a previous work (Godinho et al. 2009), only peak 1 was observed due to the limited range of wave vectors investigated. The correlation lengths $D = \lambda_x/(W\cos\theta)$ calculated are $D_1 \sim 3$ nm, $D_2 \sim 2$ nm and $D_3 \sim 14$ nm. The analysis of the

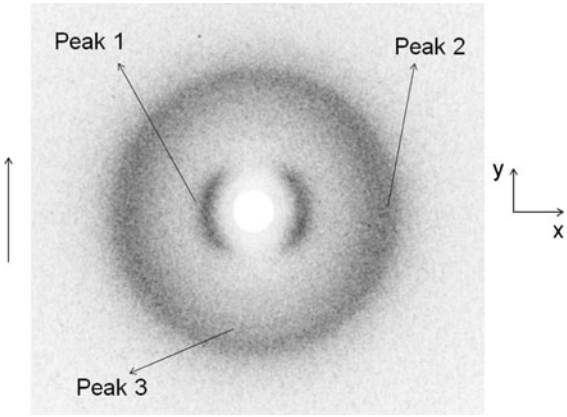

Fig. 1 X-ray diffraction pattern of the unstretched cellulose film. The *single arrow* represents the casting direction and the *double arrow* the stretching direction. Peaks 1, 2 and 3 are identified

diffraction peaks in the x–y plane indicates that peaks 1 and 2 are more intense along the x direction, which corresponds to the direction perpendicular to the casting. On the other hand we could not fully verify if peak 3 is also anisotropic with respect to the z-axis since the presence of peak 2, particularly along the x-axis direction, prevents a reliable azimuthal analysis of it. Nevertheless, visual inspection of Fig. 1 seems to indicate that this peak is preferentially located in the direction perpendicular to the casting direction. The azimuthal angle analysis of the diffracted intensity (angle φ, measured in the xy plane, starting from the x-axis, in the counterclockwise direction) of the peaks allowed us to obtain the orientational order parameters (OP). They were calculated according to Deutsch (1991), by using Eq. 1 and the azimuthal diffracted intensity $I(\varphi)$

$$\mathrm{OP} = 1 - N^{-1}\frac{3}{2}\int_0^{\pi/2} I(\varphi)\left\{\sin^2\varphi + (\sin\varphi) \times \left(\cos^2\varphi\right)\ln[(1+\sin\varphi)/\cos\varphi]\right\}d\varphi, \qquad (1)$$

where

$$N = \int_0^{\pi/2} I(\varphi)d\varphi.$$

We obtained $\mathrm{OP}_1 = 0.40 \pm 0.01$ and $\mathrm{OP}_2 = 0.29 \pm 0.01$. At this stage of the experiment (unstretched film) OP_3 was not possible to be evaluated due to the spread of peak 2.

In accordance with Godinho et al. (2009), we associate peak 1 with the distance between APC chains, preferentially oriented along the casting direction, in a "nematic-type" ordering. We propose that peak 2 is associated with the average distance between segments of the molecules that form the cellulosic matrix and links the glucose molecules. These segments were also partially oriented along the casting direction. The existence of the narrow peak 3 is particularly interesting. It indicates the existence of an ordered structure with a large correlation length ($D_3 \sim 14$ nm), which seems to be oriented perpendicular to that of the nematic-like ordering. We propose to associate this characteristic distance d_3 with a smectic-like ordering inside correlation volumes of typical dimension $(D_3)^3$ where the glucose molecules are stacked. These correlation volumes should be preferentially oriented with the normal to the smectic layers parallel to the casting direction. This aspect will become clearer when the stretched sample is analyzed in the following.

Films under stress

Let us now analyze the situation where the film is subjected to a uniaxial stress parallel to the casting direction (Fig. 3). We did not observe significant differences in the patterns obtained in the different film locations of the X-ray exposures, indicating, at least, in our experimental conditions, homogeneity of the film. As the stress increases, the order parameters of the three peaks increase, reaching values at the maximum stress applied ($\varepsilon_y = 0.40$) of $\mathrm{OP}_1 = (0.85 \pm 0.03)$, $\mathrm{OP}_2 = (0.43 \pm 0.02)$ and $\mathrm{OP}_3 = (0.82 \pm 0.01)$. This increase in the orientational order parameter of peak 1 is consistent with the results obtained by Godinho et al. (2009). Figure 4 shows the diffracted intensity as a function of q along the x (Fig. 4a) and y (Fig. 4b) axis directions. As the stretch is increased, peak 3 become more and more defined in the diffracted intensity versus q curves (Fig. 4b). The positions of the peaks were not modified by the stress. An intriguing result was obtained when we analyzed peak 2 profile as a function of the azimuthal angle φ (Fig. 4c). A hexagonal distribution of diffraction maxima could

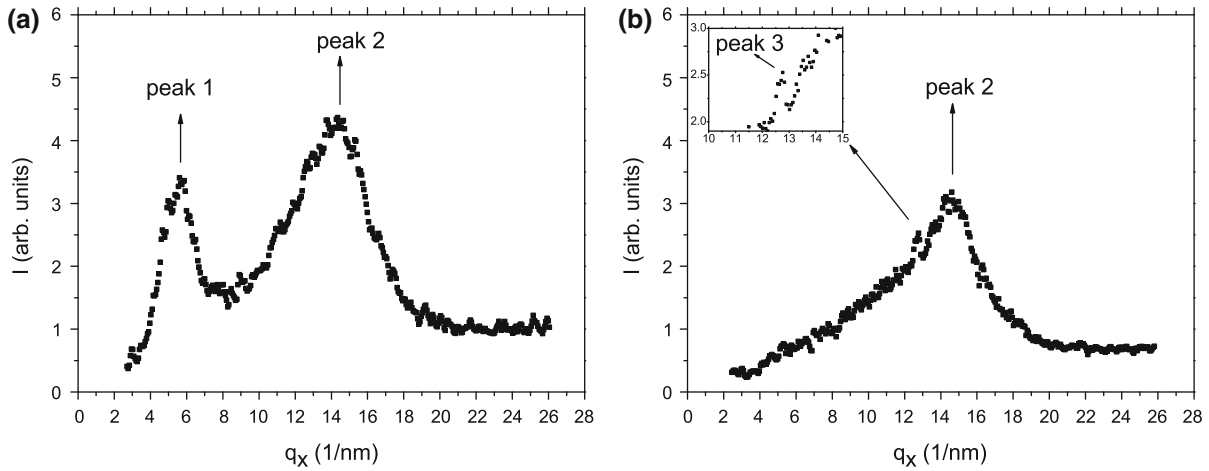

Fig. 2 X-ray diffracted intensity of unstretched cellulose film. **a** As a function of q, along the x-axis; **b** As a function of q, along the y-axis. The *insert* refers to a zoom around $q \sim 13$ nm^{-1}

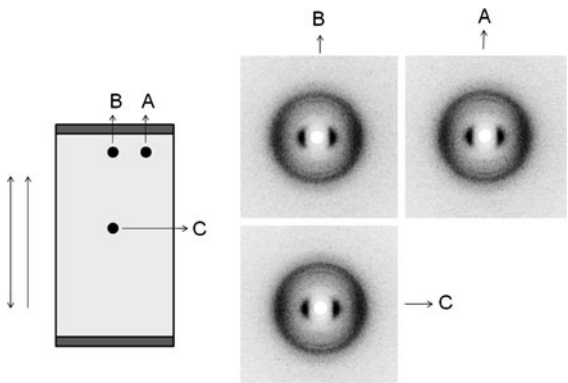

Fig. 3 Cellulose film at maximum stretch with $\varepsilon_y = 0.40$. **a** Sketch of the cellulose film under stretch and indication from where the X-ray diffraction patterns were taken. The *single arrow* indicates the casting direction and the *double arrow* the stretching direction. **b** Diffraction patterns obtained at the different film locations

be identified in the peak 2 position, which provided a hexagonal lattice parameter $d_H \sim 0.5$ nm about the same of the characteristic distance d_3. The value of d_H was obtained assuming that the diffraction peaks of hexagonal symmetry observed in the position of peak 2 ($d \sim 0.44$ nm) correspond to the (100) diffraction plane of the two-dimensional hexagonal packing, i.e., $d_H = d_{100}/\cos(\pi/6)$. The increase of the ordering of the structure under stress could be pictured as the result of the ordering of the smectic-like correlation volumes, with the corresponding ordering of the glucose molecules inside them. The cellulosic matrix that connects the glucose molecules is also oriented as a consequence of this process. The typical dimension of an extended glucose molecule is of the order of 0.5 nm and the cellobiose, composed by two glucose molecules, is the repeating building-block in the cellulosic sample. The structure proposed for the cellulosic film has to take into account the diffraction characteristic distances observed, the dimension of the cellobiose building-block, and the information that, before the casting, the system presents a cholesteric structure. We propose that in the film there is a bundle of helicoidal fiber-like structure where the cellobiose block spins around the axis of the fiber, like a string-structure in a smectic-like packing, with the pitch defined by the smectic-like layer (0.5 nm). The fibers are perpendicular to the smectic-like planes. The distance between the fibers should be of the order 1.1 nm, corresponding to peak 1 of the diffraction pattern. Since there is no evidence of chiral activity in the cellulosic films in the macroscopic scale, these bundles should have fibers with both the levogyre and dextrogyre arrangements, with equal probabilities. Without the stretch, these bundles of fibers may be warped, only with a residual orientation along the casting direction. The stretch orients the bundles along it, increasing the smectic-like and the nematic-like ordering of the fibers. Under stress, the network of molecules which connects the cellobiose blocs and forms the cellulosic matrix tends to organize their links in a hexagonal-like structure with lattice parameter commensurate to

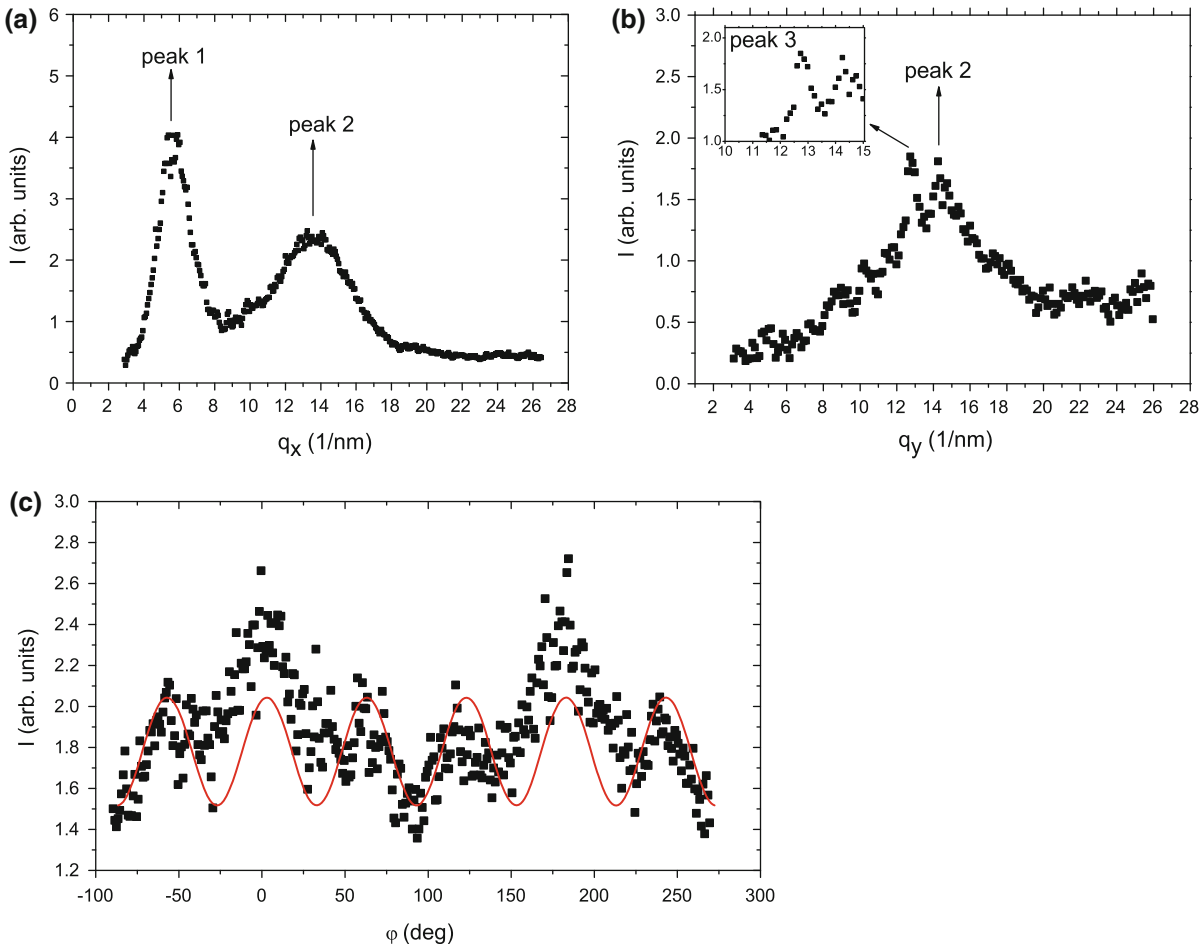

Fig. 4 X-ray diffracted intensity of stretched cellulose film at maximum stretch with $\varepsilon_y = 0.40$. **a** As a function of q, along the x-axis; **b** As a function of q, along the y-axis. The insert refer to a zoom around $q \sim 13$ nm^{-1}; **c** As a function of the azimuthal angle φ, referring to peak 2. The sinusoidal curve is only a guide for the eyes

the smectic-like structure. Kiemes et al. (2011) reported recently a theoretical study of orientationally ordered phases in two-dimensional networks of randomly cross-linked semi flexible polymers. They found a transition to an ordered state, one of them hexatic, when a critical cross-link density is achieved. Allaahyarov and Taylor (2009), Allaahyarov et al. (2010) also predicted a hexatic structure in an ionomer membrane induced by an electrical field, which, under certain conditions, persists after the removal of the field. The appearance of those diffraction peaks in our diffractogram in the condition of sample maximum stretch could be interpreted as the formation of a hexatic structure, imposed by the uniaxial stress, which acts as a *mechanical stretching field*. Moreover, the film deformation along the y-axis direction would lead to an increase in the density of the (already existent) cross-links, at least along the x-axis direction. Both processes seem to be important to the formation of the hexatic-type structure observed. When the mechanical stretching field is removed and the film is left to relax, we observed that, even after about 40 h at rest, the film does not recover its initial state. Figure 5a–c present the diffractograms of the film progressively stretched in the direction parallel to the casting with $\varepsilon_y = 0$, $\varepsilon_y = 0.29$ and $\varepsilon_y = 0.40$, and Fig. 5d, e show the diffractograms of the sample during the relaxation process, after $t_R = 21{:}21$ h, and $t_R = 41{:}10$ h, after the mechanical field removal. After these time intervals the film recovered the length corresponding to $\varepsilon_y = 0.34$ and $\varepsilon_y = 0.32$, respectively. From

Fig. 5e we obtained $OP_1 = (0.77 \pm 0.02)$, $OP_2 = (0.43 \pm 0.02)$ and $OP_3 = (0.83 \pm 0.03)$. These values clearly indicate that the film does not behave like an elastomer, keeping the memory of its high stretching condition after the stretch is released. From the nanoscopic point of view we could say that, after the smectic correlation volumes be oriented under stress, their disorientation under relaxation would cost too much energy to be done, due to the necessity of impose defects to the structure.

We will discuss now the diffractograms of the sample under consecutive stretches applied perpendicularly to the casting direction, and its relaxation. Figure 6a shows the X-ray patterns of the sample under consecutive stretches applied, with the X-ray beam positioned at the center of the film (corresponding to the position C in Fig. 6b). It is interesting to note that in this configuration (applied mechanical stretching field perpendicular to the casting direction) the sample reached values of $\varepsilon \sim 7$ without breaking, differently from the previous configuration where the sample broke at $\varepsilon \sim 0.51$. As the stretch increases, peaks 1 and 2 tend to an isotropic configuration around the z-axis, reached at $\varepsilon \sim 4$. Peak 3 is no longer observed. For larger stretches, peaks 1 and 2 come back to an anisotropic configuration, but with the average direction of the nematic

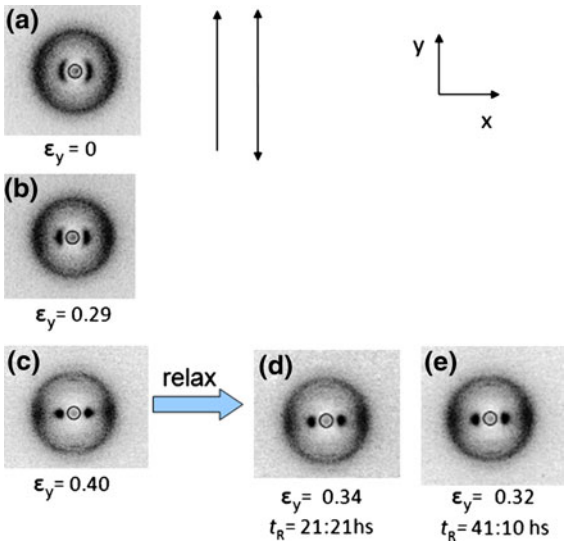

Fig. 5 X-ray diffraction patterns of the unstretched cellulose film (**a**), and stretched in the direction of the casting (**b**, **c**), and upon relaxation (**d**, **e**). The *single arrow* represents the casting direction and the *double arrow* the stretching direction

director orientation at 90° from its original (unstretched) orientation direction. Still here, peak 3 was not observed. This behavior of peak 1 is consistent with that observed in other cellulosic materials (Godinho et al. 2009). The characteristic distances associated to peaks 1 and 2 remain constant as a function of the stretch. This configuration of the stretch with respect to the casting direction destroyed the smectic ordering of the glucose molecules and, consequently, did not produced the hexatic-type structure of the bonds at the end of the process. The diffractogram obtained at maximum stretch $\varepsilon \sim 7$ shows a circular peak 1, more intense along the y-axis direction. This indicates that there are still some helicoidal fiber-like structures of cellobiose randomly oriented with respect to the z-axis. This situation is completely different from that observed in the previous configuration of the stress with respect to the casting direction where peak 1 is not observed along the y-axis. The order parameter calculated from peak 1 decreases from $OP_1 = (0.40 \pm 0.01)$ at $\varepsilon = 0$ to $OP_1 = (0.16 \pm 0.03)$ at $\varepsilon = 4$, and after increases to $OP_1 = (0.45 \pm 0.02)$ at $\varepsilon = 7$. The measured order parameter of peak 2 also decreases as a function of ε until $\varepsilon \sim 4$ and after increases to $OP_2 = (0.20 \pm 0.02)$ and remains constant. To investigate the relaxation process we performed two experiments. In the first one we left the film to relax from a stretch just before the isotropic configurations of peaks 1 and 2 were achieved at $\varepsilon = 4$ (Fig. 6a). In the second experiment, we left the film to relax from the configuration achieved with $\varepsilon = 7$ (Fig. 6a). As in the previous configuration of the stretch with respect to the casting, the relaxation process is very slow. When the film is left to relax from the condition at $\varepsilon = 4$, it tends to recover the original orientational features with peaks 1 and 2 more intense along the x-axis direction. After $t_R = 17{:}36$ h the film reached $\varepsilon = 1.92$, and after $t_R = 39{:}21$ h it reached $\varepsilon = 1.18$, $OP_1 = (0.26 \pm 0.02)$ and $OP_2 = (0.23 \pm 0.02)$. These values of the order parameters of peaks 1 and 2 correspond to those obtained during the stretching process, indicating that the film tends to return to its initial condition, but with a very long relaxation time. When the film is left to relax from the condition at $\varepsilon = 7$, it does not tend to recover the original orientational features of peaks 1 and 2. Peak 1 remains more intense along the y-axis direction. After $t_R = 60{:}29$ h the film reached $\varepsilon = 3$,

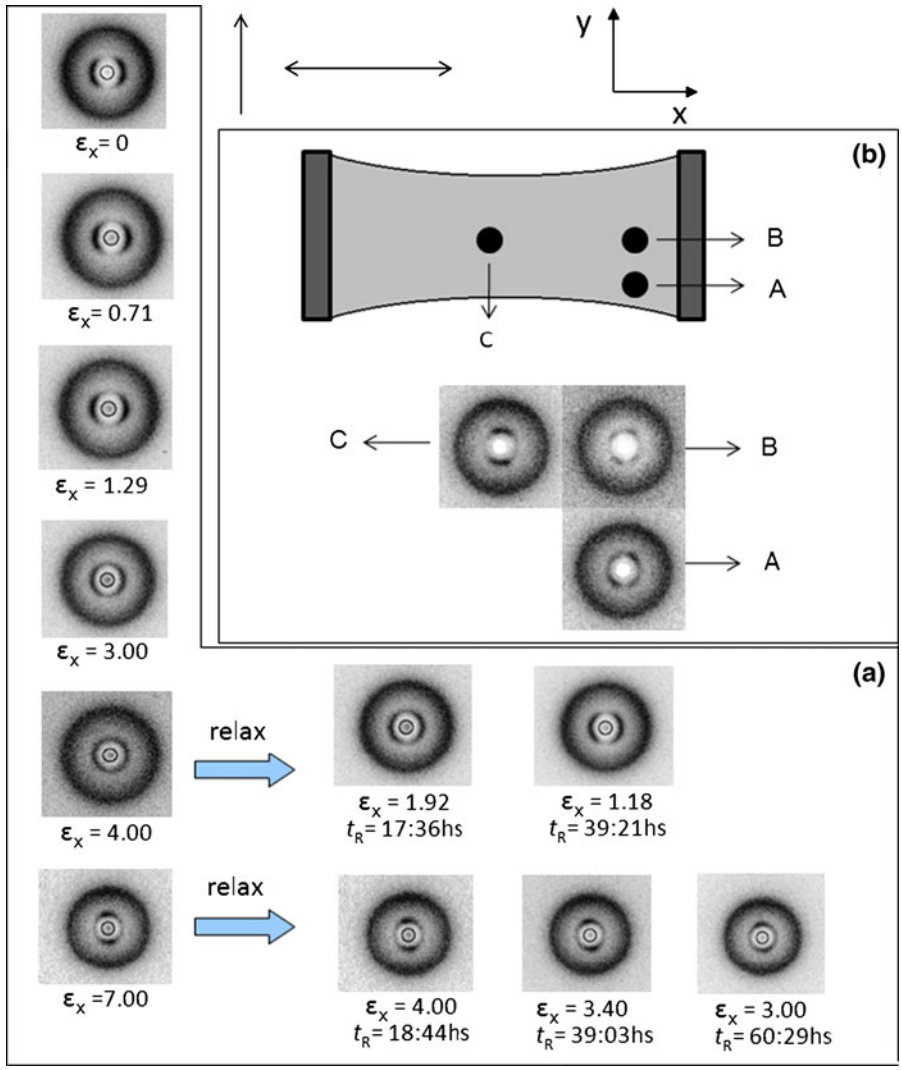

Fig. 6 **a** X-ray diffraction patterns of the cellulose film under successive stretch perpendicular to the casting direction, and upon relaxation. The *single arrow* represents the casting direction and the *double arrow* the stretching direction. **b** Sketch of the cellulose film under stretch and indication from where the X-ray diffraction patterns were taken. The *single arrow* indicates the casting direction and the *double arrow* the stretching direction. Diffraction patterns obtained at the different film locations

$OP_1 = (0.45 \pm 0.02)$ and $OP_2 \sim 0$. The structure of the film in this last scenario could be sketched as a nematic-type ordering of the helicoidal fiber-like arrangements of cellobiose, linked by molecular segments isotropically oriented with respect to the z-axis. This situation remains for a long time and an eventual formation of the previous smectic-like structure seems highly improbable since defects should be created to accommodate the smectic clusters in the arrangement present in the fresh film. To analyze the homogeneity of the film X-ray exposures were obtained with the beam probing different film positions (namely, A, B and C in Fig. 6b). Differently from the previous case of stretching parallel to the casting direction, the diffractograms obtained were different. In the borders of the film (position A) the sample director is oriented with an angle of about $+\pi/4$ with respect to the x-axis direction. On the other side of the film (position D—data not shown) the orientation of the director with respect to the x-axis is about $-\pi/4$. In the middle of the film, on the border (position B), the X-rays revealed both configurations of the director. This result seems to indicate that in the beginning of the stretching process the sample director has an orientation parallel to the casting and, under stretch perpendicular to this former direction, the director has two possibilities of reorientation, clockwise or counterclockwise with respect to the stretching direction, with the same probability. This degeneracy

is broken near the lateral borders of the film, giving rise to the patterns of Fig. 6b. In the border (position B), far from the center of the film, the pattern indicates that the directors did not complete the full rotation to achieve an orientation parallel to the stretch direction, differently from the middle of the film (position C). This is due to the boundary condition of the clamp that sustains the film and avoids its contraction. A similar result was obtained by Zubarev et al. (1999) in acrylate-based networks.

Positions B and C for the stretched film and a single position for the unstretched film were also investigated by SAXS. The obtained experimental data are shown in Fig. 7. The SAXS curves indicates that the intensity levels off at low values of q in agreement with typical Guinier behavior, indicating that there are density fluctuations on a certain large length scale. The experimental data were analyzed using a simple model that gives an average radius of gyration of the electron-density inhomogeneity (R_g) and an exponent α which indicates the characteristics

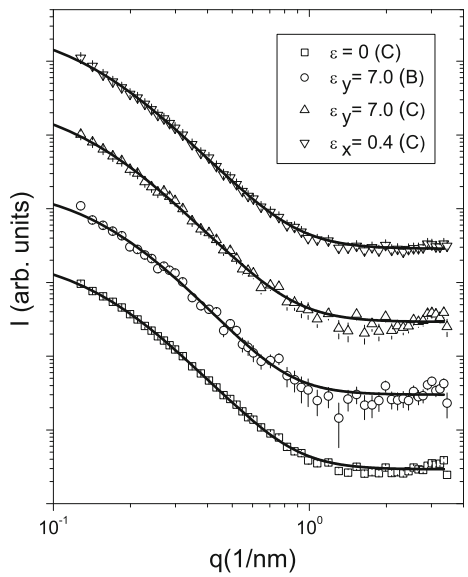

Fig. 7 Data obtained from a Small Angle X-Ray scattering experiment obtained in different film positions where the log of the scattering intensity, I, is plotted against the log of the wave number q. Superimposed on the data is the result of fits using Eq. 2 as *solid lines*. (*open square*) unstretched cellulose film, in the center of the film (position C); stretch ($\varepsilon = 7$) along the direction perpendicular to the casting (*open circle*) on the border (position B—Fig. 6b) and (*open triangle*) in the center of the film (position C—Fig. 6b); (*open inverted triangle*) stretch ($\varepsilon = 0.4$) along the direction to the casting (position C—Fig. 3)

of the aggregate. The expression used to analyse the SAXS data is given by (Schack et al. 2009):

$$I(q) = S_C \frac{1}{\left(1 + \frac{2q^2 R_g^2}{3\alpha}\right)^{\alpha/2}} + back \quad (2)$$

were S_C is an overall scale factor and *back* is a constant background. For gel-like systems the exponent α can give indications of the branching at nanoscale, given by the fractal dimension. For exponents smaller than 3 this indicates a mass fractal. For exponents higher than 3, this might indicate a surface fractal of dimensions (6-α) (Wong and Cao 1992). The fits are shown in Fig. 7 as solid lines. A summary of the results is shown in Table 1.

For all positions of the film, the SAXS data showed very similar results, independently of the stretching level and orientation. It was found a domain size of $\sim$15–17 nm. This dimension agrees with the typical size (D_3) of the smectic-type correlation volumes obtained from the analysis of peak 3 on the diffraction patters. Since the exponent is higher than 3, this domain has characteristics of a surface fractal.

The mechanical assays

Table 2 shows the values of Young's modulus, yield stress, strain and stress at break and toughness obtained at room temperature, for both configurations (parallel and perpendicular with respect to the casting direction) of the stress applied to the sample.

The film presents brittle behavior when stretched in a direction parallel to the casting, with high Young's modulus $E_{//} = 76$ MPa, low strain and high stress at break. However, when stretched in the direction perpendicular to the casting it presents ductile behavior with yield stress of 0.82 MPa. In the perpendicular configuration of the stretch with

Table 1 Results for the SAXS fitting parameters using the theoretical model represented by Eq. 2

Sample	Parameters		
	S_C	R_g [nm]	α
$\varepsilon = 0$ (position C)	0.25 ± 0.02	15.5 ± 0.6	4.01 ± 0.11
$\varepsilon_x = 7$ (position B)	0.21 ± 0.04	14.7 ± 1.5	4.21 ± 0.32
$\varepsilon_x = 7$ (position C)	0.30 ± 0.05	17.1 ± 1.4	3.84 ± 0.17
$\varepsilon_y = 0.4$ (position C)	0.31 ± 0.03	17.1 ± 0.7	3.83 ± 0.09

Table 2 Young modulus (E), yield stress, strain (ε_b) and stress at break and toughness of the cellulose (0.5% HDI/70% APC) films

Assay orientation with respect to casting	Young modulus (Mpa)	Yield stress (Mpa)	Strain at break (ε_b)	Stress at break (MPa)	Toughness (Mpa)
∥	76 ± 10	–	0.51 ± 0.05	19 ± 1	4.29 ± 0.72
⊥	21 ± 2	0.82 ± 0.09	7.73 ± 0.79	0.94 ± 0.11	5.68 ± 0.53

The symbols ∥ and ⊥ refer to the assay parallel or perpendicular to the casting direction

respect to the casting direction, the film presented a smaller Young's modulus ($E_\perp = 21$ MPa), higher strain and smaller stress at break.

The energy required to break the film (toughness) in the perpendicular configuration is 5.68 MPa, while in the parallel configuration is 4.29 MPa. These results were obtained considering that the film lateral area ($A_T = e \times 5$ mm^2) remains constant throughout the mechanical test.

The optical microscopy assays

The optical microscopy texture of the sample under crossed polarizers (casting direction parallel to the analyzer) revealed that the film is birefringent, but with a non uniform texture (Fig. 8a). The analysis of the texture under crossed polarizers leads to the macroscopic arrangement of the director sketched in Fig. 8b. There are light and dark regions which form a pattern with stripes, with a periodicity of ~4.4 μm (distance between three light regions), perpendicular to the direction of the casting. This periodic structure is originated by the shear-casting procedure. After the cast the molecular chains have a collective relaxation that results in the formation of that pattern. This morphology has been observed in other cellulose derivative films and was found to be influenced by the precursor solution composition, solvent evaporation rate, film thickness, and rate and duration of shear (Godinho et al. 2002; Wang and Labes 1992; Mori et al. 1999). The application of successive stretches in the direction of the casting (i.e., in our experimental configuration, parallel to the analyzer direction) showed that the texture of the film becomes increasingly dark. This is because the direction of the optical axis, previously created by the casting, is parallel to the analyzer direction. If the optical axis of the sample is rotated by 45° in the plane of the microscope plate the texture became bright. This result is consistent with the nanoscopic structure proposed in the previous X-ray diffraction and scattering section. The fiber-like structure where the cellobiose block spins around the axis of the fiber defines the director direction, parallel to the casting

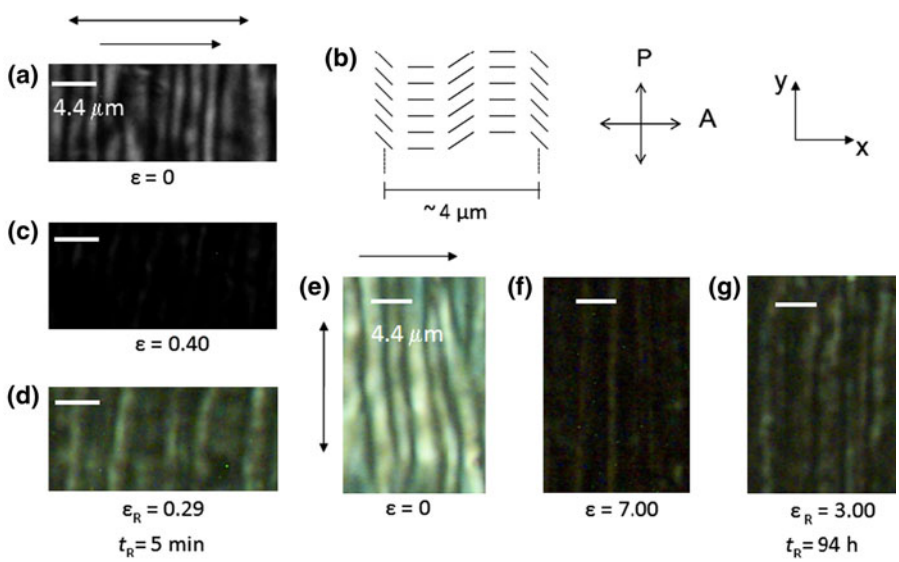

Fig. 8 Optical microscopic textures under crossed polarizers (OMP) of the film unstretched (**a**, **e**) and sketch of the director orientation (**b**); OMP of the film under stretch parallel to the casting direction (**c**), and upon relaxation (**d**); OMP of the film under stretch perpendicular to the casting direction (**f**), and upon relaxation (**g**). The *single arrow* indicates the casting direction and the *double arrow* the stretching direction

direction. As the X-ray beam probes a large portion of the sample (typical beam diameter of about1 mm) the diffraction pattern reveals the mean orientation direction of the director. Upon relaxation (initially at $\varepsilon = 0.29$ and after $t_R = 5$ min) the film did not recover the initial texture, in accordance with the X-ray results already discussed.

When the stretch is applied perpendicular to the casting direction the texture of the sample under crossed polarizers (Fig. 8e, f) becomes increasingly darker with increasing stretch, and then clearer after its relaxation (Fig. 8g). Assuming the structure depicted in Fig. 8b, the stretch along the direction perpendicular to the casting will impose a tendency of reorientation of the fiber-like arrangement parallel to the stretching direction. Depending on the location of the film analyzed and the boundary conditions imposed by the borders of the film, the fibers will tend to reorient to their local environment. This fact can explain the different X-ray patterns obtained in different film positions (Fig. 6b). At the border of the film (position A in Fig. 6b) the director, that was initially oriented in average parallel to the casting direction (x-axis), is now primarily oriented at $+\pi/4$with respect to the x-axis (counterclockwise). On the other side of the film, in a symmetric location with respect to the middle of it, we expect that the director will be primarily oriented at $-\pi/4$ with respect to the x-axis (clockwise). In the center of the film (position C in Fig. 6b), the director is oriented primarily along the y-axis. Let us look in more details the appearance of the film under stress, without the crossed polarizers. The film initially had 2 mm in length (L_0), 5 mm in width and 21 μm in thick and was stretched every 6 min until 16 mm in length, and then relaxed. Figure 9 shows the sequence of stretches of the film from $\varepsilon = 0.71$ (Fig. 9b) until $\varepsilon = 7$ (Fig. 9d), with the stress applied perpendicular to the casting direction. It is clearly observed an additional periodicity in the direction perpendicular to the casting direction. The distance (along the x-axis) between two successive stripes increases linearly with ε (Fig. 10). Under crossed polarizers these stripes are also birefringent (Fig. 11). This result indicates that the effect of the casting in the macroscopic structure of the cellulosic film is not only to impose a periodic bend organization of the local director, as sketched in Fig. 8b in its direction, but also bends this super structure in the direction perpendicular to it in a larger length scale. Upon

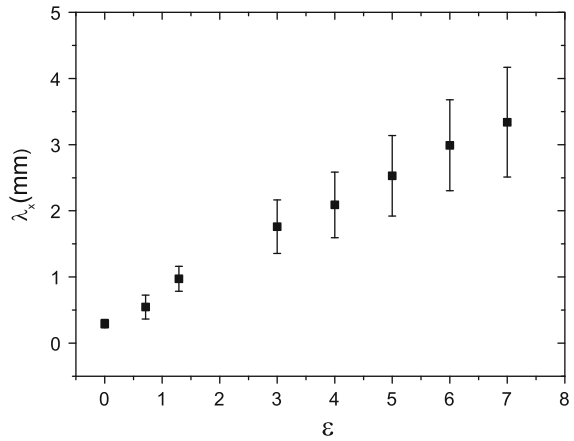

Fig. 10 Distance between two consecutive stripes along the x-axis, as a function of ε. Data corresponding to the experimental situation of Fig. 9

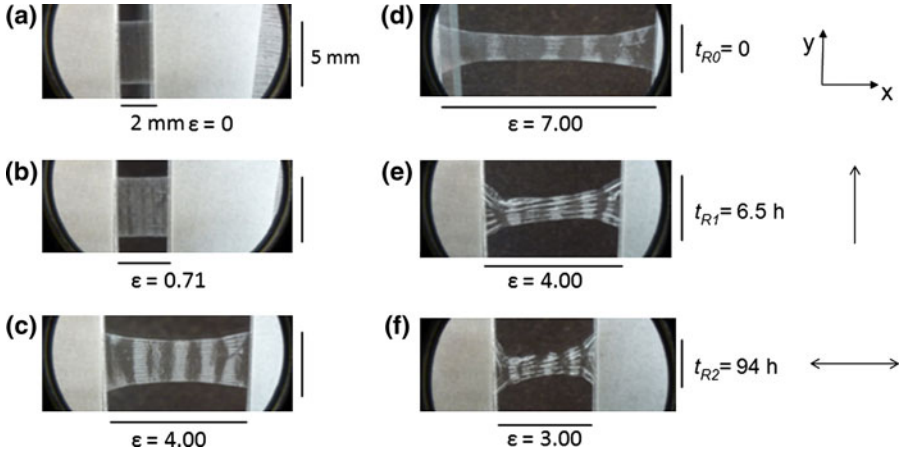

Fig. 9 Textures from optical microscopy without crossed polarizers (OM) of the film unstretched (**a**), under successive stretches (**b**, **c**, **d**) and under relaxation (**e**, **f**). Stretch perpendicular to the casting direction. The *single arrow* indicates the casting direction and the *double arrow* the stretching direction

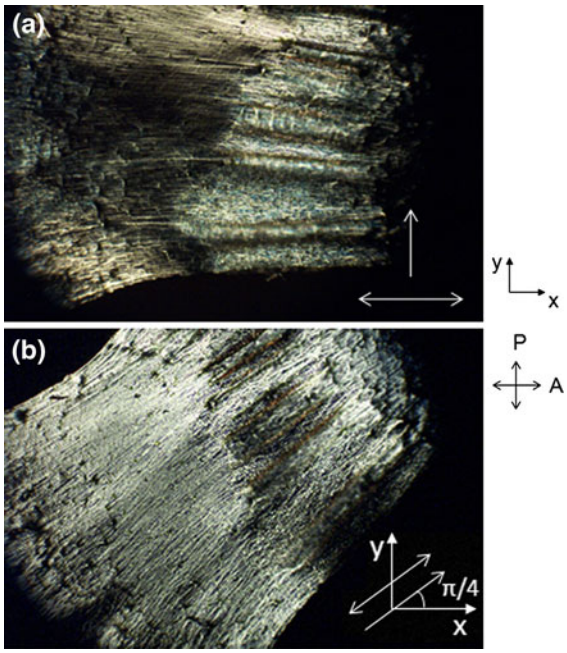

Fig. 11 Textures from optical microscopy with crossed polarizers (OMP) of the film stretched, corresponding to the sample shown in Fig. 9f: **a** Stretching direction perpendicular to the polarizer direction; **b** Stretching direction at $\pi/4$ from the polarizer direction. The *single arrow* indicates the casting direction and the *double arrow* the stretching direction

relaxation, the film takes a long time to recover its original length (Fig. 9e, f). However, its shape is strongly modified, in particular its width (direction perpendicular to the stretch), indicating the plastic behavior of the deformation.

When the film is stretched in the direction parallel to the casting direction this additional periodicity is not observed.

Conclusions

In summary, the experimental X-ray diffraction and scattering and optical microscopy observations lead us to propose the structure of the liquid crystalline cellulosic elastomers HDI-APC in free standing films without and subjected to an uniaxial stress. Our results are consistent with a framework where in the film there is a bundle of helicoidal fiber-like structure where the cellobiose block spins around the axis of the fiber, like a string-structure in a smectic-like packing, with the pitch defined by a smectic-like layer. The fibers are in average perpendicular to the smectic-like planes. These bundles should have fibers with both the levogyre and dextrogyre arrangements, with equal probabilities. Without the stretch, these bundles are warped, only with a residual orientation along the casting direction. The stretch orients the bundles along it, increasing the smectic-like and the nematic-like ordering of the fibers. Under stress, the network of molecules which connects the cellobiose blocs and forms the cellulosic matrix tends to organize their links in a hexagonal-like structure with lattice parameter commensurate to the smectic-like structure.

Acknowledgments Authors acknowledge the financial support from Fundação de Amparo à Pesquisa do Estado de São Paulo (FAPESP), Instituto Nacional de Ciência e Tecnologia de Fluidos Complexos (INCT-FCx), Conselho Nacional de Desenvolvimento Científico e Tecnológico (CNPq), Portuguese Science and Technology Foundation project PTDC/CTM/099595/2008.

References

Allaahyarov E, Taylor PL (2009) Predicted electric-field-induced hexatic structure in an ionomer membrane. Phys Rev E 80:020801(R). doi:10.1103/PhysRevE.80.020801

Allaahyarov E, Taylor PL, Löwen H (2010) Simulation study of field-induced morphological changes in a proton-conducting ionomer. Phys Rev E 81:031805. doi:10.1103/PhysRevE.81.031805

Almeida PL, Tavares S, Martins AF, Godinho MH, Cidade MT, Figueirinhas JL (2002) Cross-linked hydroxypropylcellulose films: mechanical behaviour and electro-optical properties of PDLC type cells. Opt Mater 20:97–100

Almeida PL, Kundu S, Beja D, Fonseca J, Figueirinhas JL, Godinho MH (2009) Deformation of isotropic and anisotropic liquid droplets dispersed in a cellulose liquid crystalline derivative. Cellulose 16:427–434. doi:10.1007/s10570-008-9273-x

Andresen EM, Mitchell GR (1998) Orientational behaviour of thermotropic and lyotropic liquid crystal polymer systems under shear flow. Europhys Lett 43:296–301

Bladon P, Warner M, Terentjev EM (1994) Orientational order in strained nematic networks. Macromolecules 27:7067–7075

Borges JP, Godinho MH, Martins AF, Trindade AC, Belgacem MN (2001) Cellulose-based composite films. Mech Compos Mater 37:257–264

Cidade MT, Leal CR (2003) Rheological properties of lyotropic solutions of acetoxypropylcellulose in dimethylacetamide. A comparision with the thermotropic case. Mol Cryst Liq Cryst 404:95–105. doi:10.1080/15421400390249871

Costa I, Filip D, Figueirinhas JL, Godinho MH (2007) New cellulose derivatives composites for electro-optical

sensors. Carbohydr Polym 68:159–165. doi:10.1016/j.carbpol.2006.07.029

Deutsch M (1991) Orientational order determination in liquid crystals by x-ray diffraction. Phys Rev A 44:8264–8270

Evmenenko G, Yu C-J, Kewalramani S, Dutta P (2004a) Structural characterization of thin hydroxypropylcellulose films. X-ray reflectivity studies. Langmuir 20:1698–1703

Evmenenko G, Yu C-J, Kewalramani S, Dutta P (2004b) Structural reorganization in films of cellulose derivatives in the presence of colloidal particles. Polymer 45:6269–6273. doi:10.1016/j.polymer.2004.07.015

Filip D, Costa I, Figueirinhas JL, Godinho MH (2006) Anisotropic cellulose-derived matrix for dispersed liquid crystals. Liq Cryst 33:109–114. doi:10.1080/02678290500450758

Godinho MH, Martins AF, Figueirinhas JL (1998) Composite systems for display applications from cellulose elastomers and nematic liquid crystals. Opt Mater 9:226–229

Godinho MH, Fonseca JG, Ribeiro AC, Melo LV, Brogueira P (2002) Atomic force microscopy study of hydroxypropylcellulose films prepared from liquid crystalline aqueous solutions. Macromolecules 35:5932–5936

Godinho MH, Filip D, Costa I, Carvalho A-L, Figueirinhas JL, Terentjev EM (2009) Liquid crystalline cellulose derivative elastomer films under uniaxial strain. Cellulose 16:199–205. doi:10.1007/s10570-008-9258-9

Kiemes M, Benetatos P, Zippelius A (2011) Orientational order and glassy states in networks of semiflexible polymers. Phys Rev E 83:021905. doi:10.1103/PhysRevE.83.021905

Kolpak FJ, Blackwell J (1976) Determination of the structure of cellulose II. Macromolecules 9:273–278

Kundu S, Feio G, Pinto LFV, Almeida PL, Figueirinhas JL, Godinho MH (2010) Deuterium NMR study of orientational order in cellulosic network microfibers. Macromolecules 43:5749–5755. doi:10.1021/ma100882w

Liu D, Chen X, Yue Y, Chen M, Wu Q (2011) Structure and rheology of nanocrystalline cellulose. Carbohydr Polym 84:316–322. doi:10.1016/j.carpol.2010.11.039

Mori N, Marimoto M, Nakamura K (1999) Cellulose films as alignment layers for liquid crystals: application of flow-induced molecular orientation. Adv Mater 11:1049–1051

Schack NB, Oliveira CLP, Young NWG, Pedersen JS, Ogilby PR (2009) Oxygen diffusion in cross-linked, ethanol-ewollen eoly(vinyl alcohol) gels: counter-intuitive results reflect microscopic heterogeneities. Langmuir 25:1148–1153

Siqueira G, Bras J, Dufresne A (2010) Cellulosic bionanocomposites: a review of preparation, properties and applications. Polymers 2:728–765. doi:10.3390/polym2040728

Tseng S-L, Valente A, Gray DG (1981) Cholesteric liquid crystalline phases based on (acetoxypropyl)cellulose. Macromolecules 14:715–719

Wang J, Labes MM (1992) Control of the anisotropic mechanical properties of liquid crystal polymer films by variations in their banded texture. Macromolecules 25:5790–5793

Wong P, Cao Q (1992) Correlation function and structure factor of a mass fractal bounded by a surface fractal. PRB 45(14):7627–7633

Zubarev ER, Kuptsov SA, Yuranova TI, Talroze RV, Finkelmann H (1999) Monodomain liquid crystalline networks: reorientation mechanism from uniform to stripe domains. Liq Cryst 26:1531–1540